JOURNAL OF MATERIALS SCIENCE 9 (1974) 1563–1568

Change of mosaic block size of bulk polyethylene in drawing processes

K. SUEHIRO*, T. TERASHIMA, M. TAKAYANAGI
Department of Applied Chemistry, Faculty of Engineering, Kyushu University, Fukuoka, 812 Japan

The effects of draw ratio and drawing temperature on the lattice distortion and size of mosaic block crystals during the deformation process of lamellar crystals were investigated by X-rays for bulk crystallized polyethylene samples with different thermal histories: a sample slowly cooled from the melt, a quenched sample, and an annealed sample. With a small draw ratio, the mosaic block sizes were reflected in the thermal histories of the starting samples, but they decreased rapidly on further drawing and became almost constant in the highly drawn state, being independent of the original values. However, during the drawing process, the distortion parameters did not undergo such a large change as the crystallite size. Increase in the drawing temperature resulted in an increase in crystallite size. Based on the remarkable decrease in crystallite size upon drawing, a hypothesis to explain the formation of fibre structure was proposed.

1. Introduction

Bulk crystallized polymers with spherulitic structure, which is composed of lamellar crystals growing from the central nuclei, are changed upon drawing into the fibre structure. The structural change of bulk crystallized polyethylene during the drawing process has been studied by many people using electron microscopy, X-ray crystallography, infra-red spectroscopy, birefringence etc. The change of the crystallite size of polyethylene in the necking region was first studied in detail by Kasai and Kakudo [1] from the X-ray structural view point. They revealed that the abrupt decrease of the crystallite size occurred in the necking region. Glentz and Peterlin [2] also measured the size and distortion of crystallites using samples with different thermal histories. They found that the mosaic block size in the highly drawn state did not depend on the size of the original undrawn material and was influenced only by drawing temperature. From this they concluded that lamellar crystals were broken down into mosaic blocks and this was accompanied by an unfolding of the molecular chains. These acquire high mobility and the rearrangement of the unfolded chain molecules into crystallites having a fold structure took place in the micro-necking zone. However, it is not clear how the structure of lamellar crystals changes in the course of drawing, as Glentz and Peterlin's [2] studies were only concerned with a draw ratio of 16.

In this paper the influence of drawing temperature and ratio on mosaic block size and distortion was studied by means of X-ray diffraction line widths, in particular over a wide range of draw ratios including the very early stage of deformation. The behaviour of molecular chains in the micro-necking zone, the explanation of which stays in a hypothetical stage according to the mechanisms proposed by Glentz and Peterlin [2], may be clarified in more detail by our experiments.

2. Experimental

2.1. Sample preparation

The sample used in this study was a commercial grade high-density linear polyethylene, Hizex 2200J provided by Mitsui Petro-Chemical Industries Co, Ltd with a viscosity average molecular weight ($\bar{M}_v$) of 40 000 and a degree of branching of 3 CH_3/1000 CH_2.

Three different kinds of undrawn films employed for drawing experiments were prepared by the following methods.

1. Pellets of high-density polyethylene were

*Present address: Department of Industrial Chemistry, Faculty of Science and Engineering, Saga University, Saga, 840, Japan.

melted in a laboratory press at 170°C and the sample was allowed to cool to room temperature at a cooling rate of about 1°C min^{-1}. This sample was designated the "slowly cooled" sample.

2. The molten sample was removed from the press and plunged into an ice-water bath. This sample was the "quenched" sample.

3. The quenched sample was annealed by reheating at 125°C for 24 h *in vacuo* to give the "annealed" sample.

A dumbell-shaped specimen was cut out of each film and drawn to various ratios by a tensile tester at the prescribed temperature.

2.2. X-ray diffraction measurements

The diffraction profiles were obtained with Ni-filtered Cu$K\alpha$ radiation by using a diffractometer equipped with a Geiger-Müller counter. The profiles of the $hk0$ reflections of 110, 220, 200 and 400 were obtained by the reflection method setting the draw direction of the sample parallel to the rotation axis of the goniometer. The 002 profile was obtained by the transmission method. In this case, the specimen surface was maintained at the angle $90° - \theta$ with respect to the incident and diffracted beams, where θ is the diffraction angle of the 002 reflection. The rotation axis of the sample was perpendicular to the draw direction in the latter case.

The degree of orientation of the specimens was expressed by $(180° - H°)/180°$ for the (110) and (200) planes, where $H°$ is the half-width of the intensity distribution along the Debye-Scherrer ring. Small-angle X-ray scattering was also conducted to obtain the long period of the samples.

2.3. Data analysis

The analysis of data was based on the Jones procedure [3]. The background was eliminated from the diffraction curve and the integral breadth of each reflection, B_0, was estimated. B_0 is broadened by the superposition of the diffractions by the $K\alpha_1$ and $K\alpha_2$ radiations which have very close wavelengths. The separation angle $\Delta\theta$ between the $K\alpha_1$ and $K\alpha_2$ radiations was calculated from Equation 1.

$$\Delta\theta = (\Delta\lambda/\lambda) \tan\theta \qquad (1)$$

where θ is the Bragg angle, $\lambda = 1.5418$ Å and $\Delta\lambda = 0.0038$ Å. Assuming Gaussian profile as the diffracted line shape, B_0 was converted to the integral breadth, B, associated with the $K\alpha_1$ radiation alone. This value was converted to the true integral breadth by correcting the instrumental broadening involved. Quartz powder was used as a standard material to correct for the line broadening due to the instrument itself. The diffraction profiles of quartz were analysed in a similar manner to that mentioned above and the angle of instrumental line broadening, b, was determined. In this case, a reflection produced by the $K\alpha_1$ radiation at the higher angle was used as the line shape. The true integral breadth, $\delta\beta$, was determined by the correction curve prepared from the Gaussian profile and the quartz profile.

The average mosaic block size, $\bar{D}$, and the lattice distortion parameter, g, were calculated using Equation 2, which is somewhat different in notation from Hosemann's equation [4].

$$\delta\beta_p{}^2 = \frac{1}{\bar{D}_{hkl}{}^2} + \frac{(\pi g_{hkl} p)^4}{d_{hkl}{}^2} \qquad (2)$$

where, $\delta\beta_p$ is the true integral breadth of the pth-order reflection, $\bar{D}_{hkl}$ is the average mosaic block size normal to the (hkl) plane, g_{hkl} is the paracrystalline distortion parameter, and d_{hkl} is the spacing between the (hkl) planes.

3. Results and discussion

3.1. Effect of draw ratio

The changes in mosaic block size and paracrystalline distortion parameters with increase in draw ratio at 60°C are shown in Figs. 1 and 2 for the three different samples mentioned in Section 2.1. The dimension $\bar{D}_{110}$ and the distortion parameter g_{110} were determined from the 110 and 220 reflections. The 200 and 400 reflections were used for the determination of $\bar{D}_{100}$ and g_{100}. In the undrawn state, the mosaic block size of the quenched sample was appreciably smaller than that of the slowly cooled or annealed ones; however, lattice distortions did not differ very much. Therefore, it seems that the cooling rate influences mainly the crystallite size and only slightly the quality of the crystal upon crystallization from the molten state.

Fig. 1 shows that the mosaic block size was strikingly decreased in a range of higher draw ratios in comparison with the undrawn sample and levelled off to the same constant values independent of the thermal history of the original samples, as mentioned by Glentz and

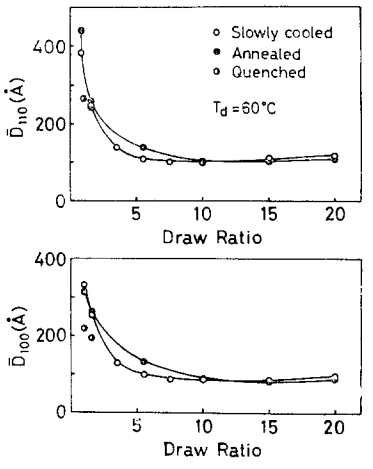

Figure 1 A plot of the mosaic block sizes (a) $\bar{D}_{110}$ and (b) $\bar{D}_{100}$ against draw ratio. Drawing temperature = 60°C.

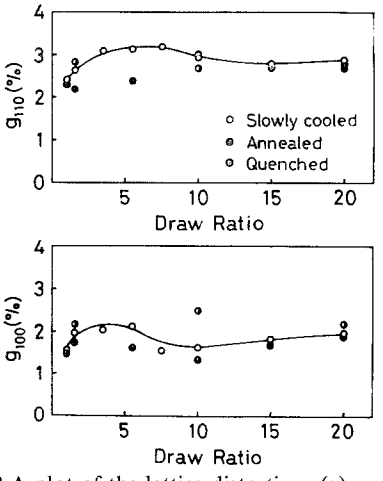

Figure 2 A plot of the lattice distortions (a) g_{110} and (b) g_{100} against draw ratio. Drawing temperature = 60°C.

Peterlin [2]. It seems that the destruction of the mosaic block is initiated at a very early stage in the drawing process and the dimensions $\bar{D}_{110}$ and $\bar{D}_{100}$ approached about 100 Å at a draw ratio of 10 times for the three samples. The degree of orientation of the (110) and (200) planes became virtually constant at the corresponding draw ratios, although the (200) plane oriented somewhat more quickly than the (110) plane as shown in Fig. 3. These results indicate that the increase in orientation corresponds well to the decrease in mosaic block size during drawing.

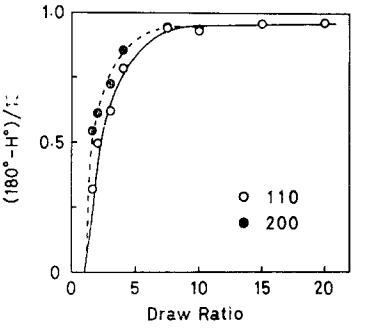

Figure 3 Degree of orientation of the (110) and (200) planes in the slowly cooled sample. $H°$ is the half-width of the intensity distribution along the Debye-Scherrer ring.

If an elliptical cylinder, the directions of the three principal axes of which coincide with those of the *a*-, *b*- and *c*-axes of the crystal, is employed as a model for the mosaic crystal block, the following relationship holds.

$$\bar{D}_{110}^{2}\left(\frac{\cos^2\phi_{110}}{\bar{D}_{100}^{2}}+\frac{\sin^2\phi_{110}}{\bar{D}_{010}^{2}}\right)=1 \qquad (3)$$

where $\phi_{110} = \tan^{-1}(a/b)$ represents the angle between the directions of (110) and (100), and a and b are the unit cell dimensions. Equation 3 can be rewritten as

$$\bar{D}_{010}=\frac{\bar{D}_{110}}{\sqrt{\left\{1+\left[1-\left(\frac{\bar{D}_{110}}{\bar{D}_{100}}\right)^2\right]\left(\frac{b}{a}\right)^2\right\}}}. \qquad (4)$$

$\bar{D}_{010}$ calculated from Equation 4 was generally larger than $\bar{D}_{100}$ (Table I). This implies that the lateral growth of a crystal has a larger tendency to develop along the *b*-axis than the *a*-axis.

The lattice distortion did not show a significant change with increasing draw ratio. g_{110} ranged between 2.2 and 3.2% and g_{100} between 1.4 and 2.5%.

TABLE I Ratio of $\bar{D}_{100}$ and $\bar{D}_{010}$ of the samples drawn at 60°C (Å)

Samples	Draw ratio							
	1	1.6	3.5	5.5	7.5	10	15	20
Slowly cooled	0.80	1.05	0.88	0.87	0.78	0.75	0.64	0.75
Annealed	0.55	1.04		0.94		0.81	0.73	0.70
Quenched	0.73	0.70				0.87		0.78

TABLE II Change of longitudinal crystallite size $\bar{D}_{001}$ by drawing at 60°C (Å)

Samples	Draw ratio							
	1	1.6	3.5	5.5	7.5	10	15	20
Slowly cooled	(250)*	(227)	162	174	175	185	200	210
Annealed	(279)	(268)		177		189	192	213
Quenched	(144)					172		214

*Values in brackets were calculated from long period L and crystallinity χ by use of a relation of $\bar{D}_{001} \simeq L\chi$.

The mosaic block size along the molecular chain, $\bar{D}_{001}$, was evaluated on the assumption that the paracrystalline distortion, g_{001}, was zero, as the atoms are linked together along this direction with covalent bonds. The results are listed in Table II. As the 002 reflection overlapped the 520 reflection at low draw ratios, the value of $\bar{D}_{001}$ for the samples with a draw ratio smaller than 1.6 was calculated from the product of the long period and the density crystallinity assuming the two phase model consists of amorphous and crystalline phases in series. The rapid decrease in $\bar{D}_{001}$ took place during slight drawing similar to $\bar{D}_{110}$ and $\bar{D}_{100}$. Decrease of the lateral and longitudinal dimensions led ultimately to a decrease in the volume of the mosaic block.

TABLE III Change of long period L by drawing at 60°C (Å)

Samples	Draw ratio					
	1	1.6	5.5	10	15	20
Slowly cooled	310	310	183	205	192	195
Annealed	331	331	205	183		185
Quenched	210			204		195

The long periods also showed a similar change in $\bar{D}_{001}$ as quoted in Table III. Strangely, the long periods became smaller than $\bar{D}_{001}$ in the highly drawn state. The longitudinal paracrystalline distortion, g_{001}, which may be greater than 0.9%, must be taken into account in order to explain this reverse relationship, as a lower limit for $\bar{D}_{001}$ is obtained in the case of $g_{001} = 0$. However, this value may be too large as the distortion along the molecular chain. In the highly drawn state, the fraction of crystal bridge compared to the surface fraction of loop or cilia might be increased. Such a model will, on average, display an increased $\bar{D}_{001}$ size while the long period cannot discriminate such an increase of crystal bridge fraction but gives the value of repeating inter-crystallite distance. This is one of the possible explanations for the phenomenon of reversed values of $\bar{D}_{001}$ and long period.

In connection with the molecular explanation for the decrease in mosaic block size at a very early stage of deformation, we consider that the stress applied for drawing at 60°C is selectively concentrated on the lamellar crystals along their plane, as the interlamellar amorphous region, including loose tie molecules and loops, shows a very low modulus due to the draw temperature high enough compared to the glass transition temperature for the amorphous region of polyethylene of −20°C. Such a concentrated stress on lamellar crystals will exert a force which then breaks down the lamellar crystals into smaller blocks. Recently, Kajiyama *et al.* [6, 7] have shown that the α_1 relaxation process associated with the intermosaic block boundary becomes remarkably increased in magnitude with increasing static strain or cycles of tensile fatigue strain. Their view supports our results obtained by X-ray measurements. It seems unnecessary to adopt the remelt and recrystallization hypothesis of Glentz and Peterlin [2], which is based on the constant size of the final crystallite with variation of original crystal size.

3.2. Effect of drawing temperature

The slowly cooled and annealed samples were drawn at various temperatures by a factor of 10. The mosaic block size and the long period were plotted against the drawing temperatures in Figs. 4 and 5, respectively. The change of the mosaic block size with drawing temperature was relatively larger in the (1 1 0) direction than in the (1 0 0). The $\bar{D}_{001}$ dimension showed a remarkable increase in the temperature range above 80°C, while the long period was gradually increased with increase in drawing temperature as in the case of polypropylene [5].

It seems that the mosaic blocks constructing the lamellar crystals of spherulites are destroyed

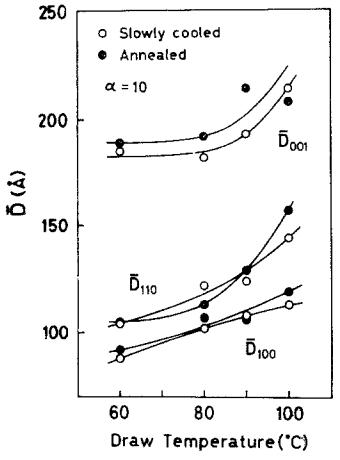

Figure 4 A plot of the mosaic block sizes $\bar{D}_{110}$, $\bar{D}_{100}$ and $\bar{D}_{001}$ against drawing temperature. Draw ratio $\alpha = 10$.

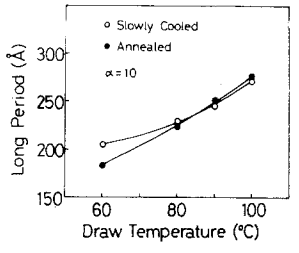

Figure 5 A plot of long period against drawing temperature. Draw ratio $\alpha = 10$.

in the necking zone by stretching, the molecular chains are drawn out from them, and recrystallize as the crystallites in the fibre structure. However, in the necking region, the microstructure will be heterogeneous in comparison to the melt, as the unbroken crystals and already drawn out chains are co-existant. The supply of molecular chains from the original mosaic block crystals may not be sufficient to grow large crystals. Consequently, the mosaic block size becomes considerably smaller after drawing in comparison with its original value before drawing as seen in the data of Figs. 1 and 4. Peterlin's hypothesis that the original crystallite is melted and recrystallized to form the fibre structure does not clearly explain this relationship. The process of remelt and recrystallization during the drawing process is acceptable for explaining the invariance of the long periods of fibre from the original samples of different histories, as the long periods may be uniquely determined by the drawing temperature. However, Peterlin's view encounters difficulties in explaining the decrease of mosaic block size as mentioned above. According to our theory, if the unfolded extended chain is released from the restraining force associated with intermolecular potential, it will refold to form a crystallite, the size of which will be uniquely determined by the drawing temperature. This mechanism also satisfies the widely accepted fibre structure of sequential arrangement of crystallites interconnected by tie molecules. Mechanically unfolded isolated extending chain will be buried by the folded crystallites which have been released from the constraining force for extension.

The main feature of our theory of the formation of fibre structure is taking into account the mechanical work exerting on the lamellar crystals to be unfolded, while Peterlin's hypothesis considers the heat generated which melts the mosaic blocks of lamellar crystal to form recrystallized crystallites in the fibre structure. For the thickness of crystallite in the fibre structure, the effect of drawing temperature on the thickness of crystallite in the fibre structure is virtually the same in both hypotheses. The higher the drawing temperature, the larger the crystallite thickness needed to stabilize the crystallite against the increasing thermal motions of molecules in the crystal. Maruyama *et al.* [8] succeeded in deriving a general equation which phenomenologically describes the deformation process from the spherulitic structure to the typical fibre structure based on the true stress and true strain relationship. To explain the meaning of the equation, it was necessary to assume the hypotheses mentioned here. Our view on plastic deformation of bulk crystallized polymers is, therefore, entirely based on the superposition of micro stress-strain deformation mechanisms in various parts of lamellar crystals, which is preferable for explaining the remarkable decrease of mosaic block size in the initial stage of deformation in comparison with the remelt-recrystallization hypothesis.

References

1. N. KASAI and M. KAKUDO, *J. Polymer Sci. A* **2** (1964) 1955.
2. W. GLENTZ and A. PETERLIN, *ibid A-2* **9** (1971) 1243.
3. F. W. JONES, *Proc. Roy. Soc.* **A166** (1938) 16.
4. R. HOSEMANN, *J. Polymer Sci. C* **20** (1967) 1.
5. F. J. BALTÁ-CALLEJA and A. PETERLIN, *ibid A-2* **7** (1969) 1275.

6. T. KAJIYAMA, T. OKADA, A. SAKODA and M. TAKAYANAGI, *J. Macromol. Sci.* **B7** (1973) 583.
7. T. KAJIYAMA, T. OKADA and M. TAKAYANAGI, *ibid* **B8** (1974) 35.
8. S. MARUYAMA, K. IMADA and M. TAKAYANAGI, *Int. J. Polymeric Mater.* **1** (1972) 211.

Received 7 February and accepted 25 March 1974.